

Robust control of solar plants with distributed collectors [★]

Cristina M. Cirre* José Carlos Moreno* Manuel Berenguel*
José Luis Guzmán*

* *Dep. Lenguajes y Computación, University of Almería, Almería,
Spain (e-mail: {ccirre,jcmoreno,beren,joguzman}@ual.es)*

Abstract: This paper presents a robust control scheme for a distributed solar collector (DSC) field. As DSC are systems subjected to strong disturbances (mainly in solar radiation and inlet oil temperature), a series feedforward is used as a part of the plant, so that the system to be controlled has one input (fluid flow) and one output (outlet temperature) as the disturbances are partially compensated by the series feedforward term, so that the nonlinear plant is transformed into an uncertain linear system. The Quantitative Feedback Theory technique (QFT) has been used to design a control structure that guarantee desired control specifications, as settling time and maximum overshoot, under different operating conditions despite system uncertainties and disturbances. To account for input and output constraints, both an antireset-windup mechanism and a reference governor have been used. Experimental tests are presented.

Keywords: Robust control, process control, feedforward control, quantitative feedback theory, solar plants.

1. INTRODUCTION

The main difference between a conventional power plant and a solar plant is that the primary energy source, while being variable, cannot be manipulated. The objective of the control system in a distributed solar collector field (DSC) is to maintain the outlet oil temperature of the loop at a desired level in spite of disturbances such as changes in the solar irradiance level (caused by clouds), mirror reflectivity, or inlet oil temperature. The means available for achieving this is via the adjustment of the fluid flow and the daily solar power cycle characteristics are such that the oil flow has to change substantially during operation. This leads to significant variations in the dynamic characteristics of the field, which cause difficulties in obtaining adequate performance over the operating range with a fixed parameter controller (Camacho et al., 1997, 2007a,b). As described in (Camacho et al., 2007a,b), the control problem of this changing dynamics has been mainly addressed ranging from classical proportional- integral-derivative control (PID), feedforward control (FF), model based predictive control (MPC), adaptive control (AC), gain-scheduled control (GS), cascade control (CC), internal model control (IMC), time delay compensation (TDC), optimal control (LQG), nonlinear control (NC), robust control (RC), fuzzy logic control (FLC) and neural network controllers (NNC). However, although some robust control techniques have been tested, there are not as many results for this control problem from a robust point of view as for other control strategies. Robust control tries to apply principles and methods that allow the discrepancies between the model and the real process to be explicitly considered. There are many techniques for designing feedback systems with a

high degree of robustness, some of which are commented in (Camacho et al., 1997) in the scope of the control of solar plants. The application of a robust optimal LQG/LTR control scheme is described in (Rubio et al., 1996). In (Ortega et al., 1997), a controller based on the H_∞ theory was developed and successfully tested. In (de la Parte et al., 2008) the application of three predictive sliding mode controllers is presented, using a first order plus dead time model for controller tuning purposes. The approach used in this work takes advantage of the assurance of high stability margins in the face of a norm bounded perturbation and uses the feedforward controller in series with the developed controller.

This paper is focused on obtaining new contributions in the robust control problem of DSC, where this work is based on the preliminary ideas developed in (Cirre et al., 2003) and (Cirre et al., 2004) and those presented in (Moreno et al., 2002) for the greenhouse climate control problem. Concretely, this work deals with the design of a robust PID controller to control the outlet oil temperature of a DSC loop using the QFT technique (Horowitz, 1993) and both an antireset-windup mechanism and a setpoint supervisory system to avoid input and output constraints violation.

The paper is organized as follows. Section 2 is devoted to describe the distributed solar collector field. The control problem is presented in section 3. The next section is focused on describing the approximated uncertain system model, the robust controller design and the reference governor. Section 5 is dedicated to describe the experimental tests. Finally, some conclusions and future works are summarized.

* The authors gratefully acknowledge CIEMAT and the Spanish Ministerio de Ciencia e Innovación (DPI2007-66718-C04-04).

2. PLANT DESCRIPTION

The ACUREX thermosolar plant is located at the Plataforma Solar de Almería (PSA), a research centre of the Spanish Centro de Investigaciones Energéticas Medioambientales y Tecnológicas (CIEMAT), in Almería, Spain. The plant is schematically composed of a distributed collector field, a recirculation pump, a storage tank and a three-way valve, as shown in Figure 1 and 2. The distributed collector field consists of 480 eastwest-aligned single-axis-tracking parabolic trough collectors, with a total mirror aperture area of 2672 m², arranged in 20 rows forming 10 parallel loops (see Figure 1). The parabolic mirrors in each collector concentrate the solar irradiation on an absorber tube through which Santotherm 55 heat transfer oil is flowing. For the collector to concentrate sunlight on its focus, the direct solar radiation must be perpendicular to the mirror plane. Therefore, a sun-tracking algorithm causes the mirrors to revolve around an axis parallel to the tube. Oil is recirculated through the field by a pump that under nominal conditions supplies the field at a flow rate of between 2 l/s (in some applications 3 l/s) and 12 l/s. As it passes through the field, the oil is heated and then the hot oil enters a thermocline storage tank, as shown in Figure 2. The hot oil can also feed a heat exchanger directly to produce steam for electricity generation in a turbine or as the primary energy source in a solar desalination plant. The cold field inlet feed oil is taken from the bottom of the storage tank (Álvarez et al., 2009). A three-way valve allows the oil to recirculate through the field until the outlet temperature reaches nominal and the oil can be sent into the storage tank. A complete detailed description of the ACUREX plant can be found in (Camacho et al., 1997).

3. THE CONTROL PROBLEM

For electricity generation process (oil temperature around 285°C) or for the use in a desalination plant (oil temperature more than 160°C), the oil is extracted from the top of the tank and it is convenient to avoid fluctuations at this position. The control problem of the solar collector field is to keep the outlet temperature T_{out} (°C) as nearest as possible to a desired temperature (temperature set point or reference, T_{ref} in °C) established manually by the operator (using the reference governor explained in the next section as a decision-aid system) according to the process (electricity production or desalination plant) and to the constraints of the plant for security reasons. For instance, one of these constraints consists in avoiding to reach an outlet temperature of 70 °C or 80 °C over the inlet temperature (T_{in} in °C) coming from the top or the bottom of the tank. Furthermore, variations in solar radiation I (W/m²) because of passing clouds, the natural daily radiation cycle, and changes in the inlet temperature due to the oil stratification inside the tank and in the ambient temperature (T_{amb}) cause variations in the outlet temperature. These disturbances cannot be manipulated, and as commented above, in order to reach the desired outlet temperature, the volumetric flow rate (q in l/s) of the oil propelled by the pump is manipulated. Although the series feedforward controller developed in (Camacho et al., 1997) has been used to compensate for

the disturbances effects (figure 3), a different operating point is obtained depending on the disturbances and flow value, where the characteristic gains, time delays, and time constants change (Camacho et al., 1997). Therefore, the proposed robust controller must be able to reach the desired specifications despite these system variations.



Fig. 1. ACUREX solar plant

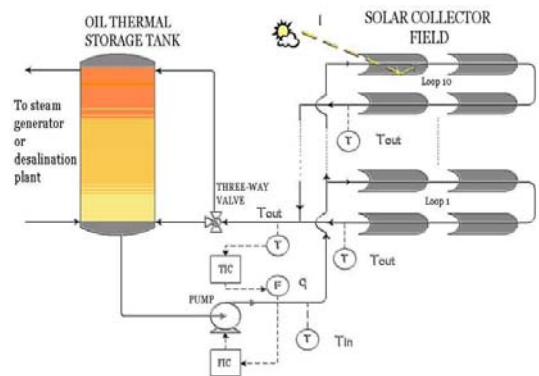


Fig. 2. Simplified layout of the ACUREX plant

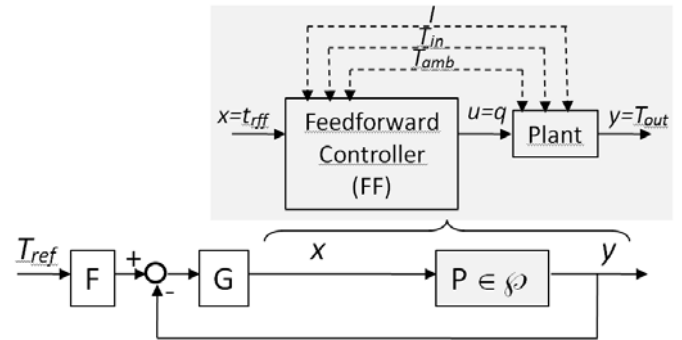


Fig. 3. A 2DoF control system with uncertain plant including the series feedforward controller

4. MODELLING ISSUES AND ROBUST CONTROL DESIGN

4.1 Uncertain model

As described in (Camacho et al., 1997), DSC dynamics can be approximated by low-order linear descriptions of the plant (as is usually done in the process industry) to model the system around different operating conditions and to design diverse control strategies without accounting for system resonances (Meaburn and Hugues, 1993; Meaburn, 1995; Camacho et al., 1997; Álvarez et al., 2007)). Thus, different low-order models are found for different operating

points mainly due to fluid velocity and system disturbances. Using the series feedforward controller (Camacho et al., 1997) (improved in (Roca et al., 2008)) a nonlinear plant subjected to disturbances is treated as an uncertain linear plant with only one input (the reference temperature to the feedforward controller, T_{rff}). In this way, the disturbances affecting the plant are not explicitly taken into account, as the feedforward term partially compensates them. Hence, for each operation point and using the series feedforward, a model of the plant is estimated, obtaining a set of plant models with the same structure where all the operating points are included as the parameters values vary from a model to another so that the ACUREX field model can be expressed as a model with uncertain parameters. In order to compute the set of LTI plant models the simulator package in (Berenguel et al., 1994) and the real plant have been used to perform reaction curve and PRBS (pseudo random binary sequence) tests in different operating conditions. After performing an analysis of the frequency response, it is observed that the characteristics of the system (time constants, gains, resonance modes, ...) depend on the fluid flow rate as expected (Camacho et al., 1997; Álvarez et al., 2007). Therefore, in order to control the system with a fixed-parameter controller, the following model has been used

$$\varphi(s) = \left\{ P(s) = \frac{k\omega_n^2}{s^2 + 2\xi\omega_n s + \omega_n^2} e^{-\tau_d s} : \xi = 0.8, \right. \\ \left. \tau_d = 39s, \omega_n \in [0.0038, 0.014] \text{rad/s}, k \in [0.7, 1.05] \right\}, \quad (1)$$

where the chosen nominal plant is $P_0(s)$ with $\omega_n = 0.014$ rad/s and $k = 0.7$.

To obtain a controller fulfilling a set of performance and stability specifications, so that all the uncertainty in the process is taken into account in the design process, a robust control technique must be used. In this sense, QFT (Horowitz, 1993) will be used in this next section.

4.2 Robust control design

As well-known, QFT is a methodology to design robust controllers based on frequency domain (Horowitz, 1993). This technique allows designing robust controllers which fulfil some minimum quantitative specifications considering the presence of uncertainties in the plant model. With this theory, it is established that the final aim of any control design must be to obtain an open-loop transfer function with the suitable bandwidth in order to sensitize the plant. The Nichols chart is used to achieve a desired robust design over the specified region of plant uncertainty where the aim is to design a compensator $G(s)$ and a prefilter $F(s)$ (if it is necessary) according to Figure 3, so that performance and stability specifications are achieved for the family of plants.

Thus, once the uncertain model has been obtained, the specifications must be determined on time domain and translated into the frequency domain for the QFT design. In this case, the tracking and stability specifications were established (Horowitz, 1993). By tracking specification the effect of the uncertainties will be reduced. It is only necessary to impose the minimum and maximum values for the magnitude of the closed-loop system in all frequencies. With respect to the stability specification, the desired gain (GM) and phase (PM) margins are set.

The tracking specifications were required to fulfill a settling rise time between 5 and 35 minutes and an overshoot less than 30% after 10-20°C setpoint changes for all operating conditions (realistic specifications, see (Camacho et al., 2007a,b)). These specifications are translated to the following frequency conditions using the QFT framework obtaining

$$|B_l(j\omega)| \leq \left| F(j\omega) \frac{P(j\omega)G(j\omega)}{1 + P(j\omega)G(j\omega)} \right| \leq |B_u(j\omega)| \quad (2) \\ \forall \omega > 0, \forall P \in \varphi$$

where $B_l(j\omega)$ and $B_u(j\omega)$ are the minimum and maximum values for the magnitude of the closed-loop system in all frequencies to fulfill tracking specifications.

For stability specification, the following condition must be fulfilled

$$\left| \frac{P(j\omega)G(j\omega)}{1 + P(j\omega)G(j\omega)} \right|_{dB} \leq \delta(\omega) = 3.77 \quad (3) \\ \forall \omega > 0, \forall P \in \varphi$$

in order to guarantee a phase margin of 35 degrees for all operating conditions.

In order to design the compensator $G(s)$ the tracking specifications in (4) are transformed into

$$\left| \frac{P(j\omega)G(j\omega)}{1 + P(j\omega)G(j\omega)} \right| \leq |B_u(j\omega)| - |B_l(j\omega)| = \Delta(\omega) \quad (4) \\ \forall \omega > 0, \forall P \in \varphi$$

Table 1 shows the specifications in (4) for each frequency in the set of design frequencies W . Using these specifications, the stability specification in (3), system uncertainties, tracking and stability boundaries are computed using the algorithm in (Nordgren and Franchek, 1994). The computed boundaries are shown in Figure 4, as well as stability and tracking boundaries with the shaped $L_0(j\omega) = G(j\omega)P_0(j\omega)$ satisfying all of them for all frequencies in W .

Table 1. Tracking specifications for the G compensator design

ω (rad/s)	0.0006	0.001	0.003	0.01
$\delta(\omega)$	0.55	1.50	9.01	19.25

The resulting compensator $G(s)$ synthesized in order to achieve the stability specifications in (3) and the tracking specifications in (4) is the following PID-type controller

$$G(s) = 0.75 \left(1 + \frac{1}{180s} + 40s \right) \quad (5)$$

In order to satisfy the specifications in (2), the prefilter $F(s)$ must be designed, where the synthesized prefilter is given by

$$F(s) = \frac{0.1}{s + 0.1} \quad (6)$$

Figure 5 shows that the tracking specifications (2) are fulfilled for all uncertain cases. Note that the different appearance of bode diagrams in closed loop for five operating conditions is due to the changing root locus of $L(s)$ when the PID is introduced. The time response for these operation conditions is shown in Figure 6.

Assuming the 2DoF controller given by compensator $G(s)$ (5) and prefilter $F(s)$ equation (6), stability problems can

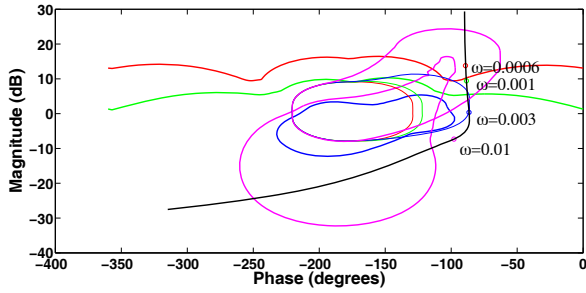


Fig. 4. Tracking and stability boundaries with the designed $L_0(j\omega)$

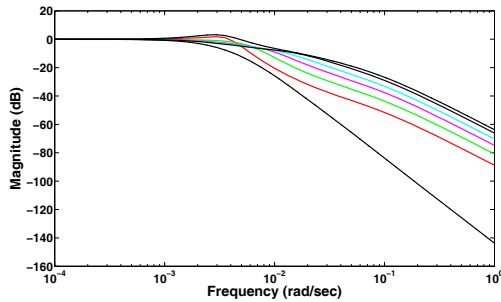


Fig. 5. Tracking specifications (dashed-dotted) and magnitude Bode diagram of some closed loop transfer functions

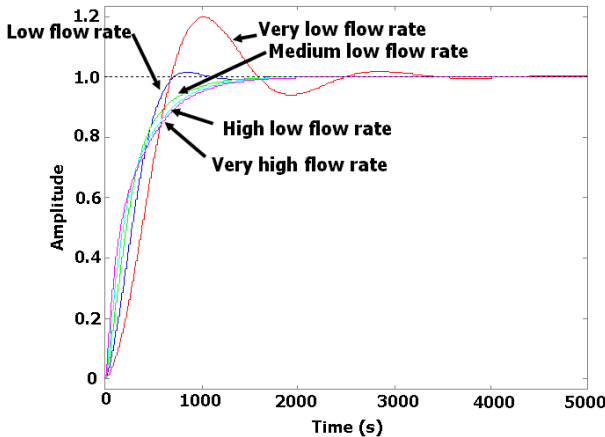


Fig. 6. Time step responses for some operation conditions

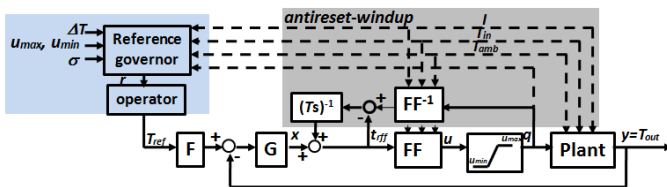


Fig. 7. Control scheme with antireset-windup and reference governor

appear when oil flow rate saturates at $u_{min} = 2$ l/s or $u_{max} = 12$ l/s. Moreover, the absolute stability cannot be assured using QFT due to the flow-outlet temperature dependent time delay present in the process (Horowitz, 1993) (that is small when compared to the main time constant of the system). Therefore, two strategies have

been included to account for this problem: the use of an antireset-windup mechanism and the development of a reference governor to avoid flow saturation to be used as a support decision tool by the operator.

Figure 7 shows the antireset-windup scheme used in this paper (where T is the tracking constant of the antireset-windup term). This mechanism is a soft modification of the classical antireset-windup (Åström and Hägglund, 2005). In this case, the saturation is located between the feedforward term and the plant, and the compensator is placed before the feedforward term. Thus, when the actuator saturates to u_{max} (or u_{min}) value the corresponding feedforward term input, T_{rff} , which would provide an output u_{max} (or u_{min}) taking into account the measurable instantaneous solar irradiance, is computed using the term FF^{-1} that implements the inverse of the feedforward compensator.

The second element used to try to avoid control signal saturation and to maximize outlet power taking into account the security constraints is the use of a reference governor to support the decision of the operator on the actual setpoint (also shown in figure 7). The reference governor supplies the reference r taking into account the actual operating conditions (outlet temperature, inlet temperature, solar radiation, ambient temperature, and both the maximum allowed temperature gradient $\Delta T = (T_{out} - T_{in})$ and the mirrors reflectivity σ). This reference is used by the operator in order to take decisions about setpoint changes. This element uses static models of the DCS based on mass and energy balances Camacho et al. (1997); Cirre et al. (2004) including measurable disturbances, so that, the reference should have to be filtered using a low-pass filter (in the case treated in this paper, this role is also adopted by prefilter F of the 2DoF control structure). Another advantage when using the reference governor is that is a very useful tool for giving adequate setpoints during one of the most difficult parts of the operation, the startup, where control signals are usually saturated during long intervals and the inlet temperature suffers from the largest changes during the operation due to the existence of cold oil inside the tubes.

Using the energy balance equation given by (7) and the developments in (Camacho et al., 1997), a function relating a temperature reference with the actual operating conditions, the control signal constraints and the allowed temperature gradient has been obtained. In (7), Q_{in} is the input power (W) and Q_{loss} is the power related to losses, that can be expressed as a function of the difference between the outlet and ambient temperatures. In equation (7) the energy collected by the system per time unit is given by $\dot{m}\Delta h$, \dot{m} being the mass flow rate (kg s^{-1}) and Δh the input-output specific energy gradient (J kg^{-1}). The specific enthalpy of the oil can be obtained using equation (8) from the oil specific heat c_p ($\text{J kg}^{-1} \text{ }^\circ\text{C}^{-1}$), that is a function of temperature in Celsius degrees.

$$Q_{in} - Q_{loss} = \dot{m}\Delta h; \quad (7)$$

$$Q_{in} = \eta\sigma A_{cor} I_{cor}; \quad Q_{loss} = H_l(T_{out} - T_{amb})$$

$$h = c_p T; \quad c_p = 1820 + 3.478T; \quad \rho = 903.16 - 0.672T_{in} \quad (8)$$

Q_{in} depends on the peak optical efficiency η of the collectors, the mirror's reflectivity σ , the effective reflecting surface A_{cor} and the effective corrected irradiance onto

the collector surface I_{cor} (Ajona, 1998). A_{cor} and I_{cor} are a function of the incidence angle between the solar rays and the collector normal, that is continuously updated depending on the solar hour and the date to obtain A_{cor} and I_{cor} from the total reflecting surface and the direct solar radiation respectively. Q_{loss} depends on a global losses function H_l ($W\ ^\circ C^{-1}$) that has been estimated from experimental data (Carmona, 1985) given by:

$$H_l = c_1 \left(\frac{T_{out} + T_{in}}{2} - T_{amb} \right) - c_2; \quad (9)$$

$$c_1 = 0.055, c_2 = 0.006133.$$

The mass flow rate \dot{m} can be obtained from the measured volumetric flow rate and using ρ in equation (8), that is the oil density ($kg\ m^{-3}$), function of temperature. Combining (7) and (8) a second order algebraic equation of the form $Ar^2 + Br + C = 0$ can be obtained that allows obtaining a desired reference temperature r (substituting T_{out} by r) as a function of a given mass flow rate and measurable disturbances, with $A = 3.478\dot{m} + (c_1/2)$, $B = 1820\dot{m} + c_1(T_{in}/2) - (3/2)c_1T_{amb} - c_2$, and $C = -(\eta\sigma A_{cor}I_{cor} + (c_1(T_{in}/2) - T_{amb}) + c_2)T_{amb} + \dot{m}T_{in}(1820 - 3.478T_{in})$.

The solution of the second order algebraic equation provides both a positive and a negative real solutions, the first one used as reference. Nevertheless, this solution does not guarantee constraints in ΔT and \dot{m} (or q). So, the solution obtained in the previous step is used as an initial solution to iterate the mass flow rate values and the associated reference temperature till these constraints are achieved. If the thermal losses are considered to be negligible, the solution can always be found and in very few iterations and even a look-up table can be used relating mass flow rates with temperatures maximizing outlet temperature while not violating the constraints. If thermal losses are taken into account, an easy quadratic programming problem can be solved. The solar radiation used for calculations is filtered (using a mean filter with forgetting factor) and also the obtained reference to avoid sudden changes in the reference due to passing clouds.

As has been pointed out, the obtained value of the reference is used by the operator to take decisions about the setpoint. Notice that the obtained reference is always changing without a determined profile, so that steady state errors can appear. So, due to the following reasons, step changes in setpoints are introduced: operators are familiarized with these kind of setpoint changes, negligible steady state errors can be obtained using controllers including at least one integrator and the specifications of the most common controllers, like QFT in this paper, are always related to step changes in setpoints. Figure 8 shows an example of the reference obtained by the reference governor and the setpoint used by the operator, including also the outlet temperature and oil flow demanded when operating with the QFT-based control scheme described in this paper. Notice that during start-up the operator took a more conservative setpoint control policy than the reference governor.

5. EXPERIMENTAL RESULTS

This section presents some experiments performed at the ACUREX solar plant using the control strategy presented in the previous section. Furthermore, the benefits of the

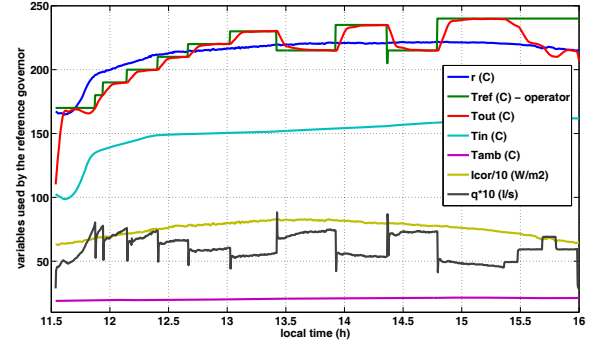


Fig. 8. Results provided by the reference governor to avoid input and output constraints violation

antireset-windup scheme in the start up phase are compared with the same controller without an antireset-windup term (and a bad management of the setpoint during this phase). In order to prove the fulfillment of the tracking and stability specifications of the control structure, experiments have been performed under several operating points and under different conditions of disturbances. Only representative results are shown in this paper. The outlet controlled has been the loop with the maximum temperature for all the experiments. The sampling time was chosen equal to 15 seconds.

Figure 9 shows an experiment with the robust controller but without antireset-windup. At the beginning of the experiment, the flow is saturated until the outlet temperature is higher than the inlet one (the normal situation during the operation). This situation always appears due to the oil resident inside the pipes is cooler than the oil from the tank. Once the oil is mixed in the pipes, the outlet temperature reaches a higher temperature than the inlet one. During the start up, steps in the reference temperature are made until reaching the nominal operating point. The overshoot at the end of this phase is $18\ ^\circ C$ approximately, and thus the specifications are fulfilled. Analyzing the time responses, a settling time between 11 and 15 minutes is observed at the different operating points. Therefore, both time specifications, overshoot and settling time are properly fulfilled. Disturbances in the inlet temperature (from the beginning until $t = 12.0$ h), due to the temperature variation of the stratified oil inside the tank, are observed during this experiment and correctly rejected by the feedforward action.

Finally, in order to check the behavior of the control structure in the most complicated situation, changing radiation due to a clouds passing, a new test under these conditions is presented in Figure 10. When the step responses are analyzed, it can be seen that the settling time is between 12 and 30 minutes in this case, and the overshoot is under 15 % in all cases. Hence, the tracking and stability specifications are fulfilled for a cloudy day despite the system uncertainty in presence of different operating points. At $t = 12.39$, a change in the inlet temperature is observed due to a variation in the three-way valve, causing an increment of $6^\circ C$ in the outlet temperature. However, the error was reduced in 17 minutes thanks to the feedforward action. From 14 hours to the end of the test, the solar radiation was

too low and it was impossible for the controller to track the proposed reference (the operator did not changed the reference accordingly with that suggested by the reference governor).

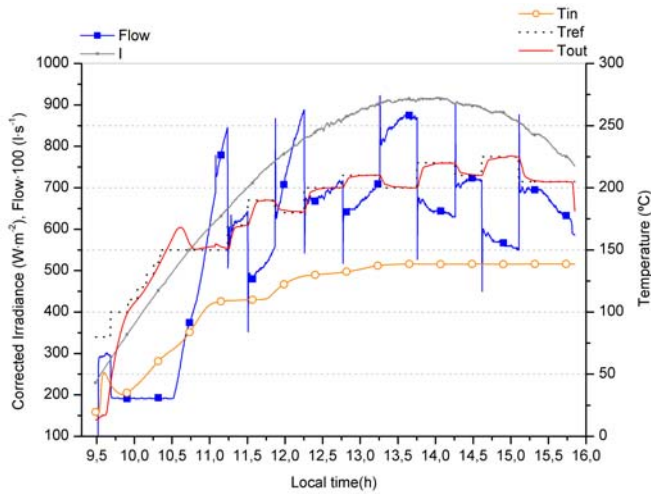


Fig. 9. Test with PID without antireset-windup (24/03/2009)

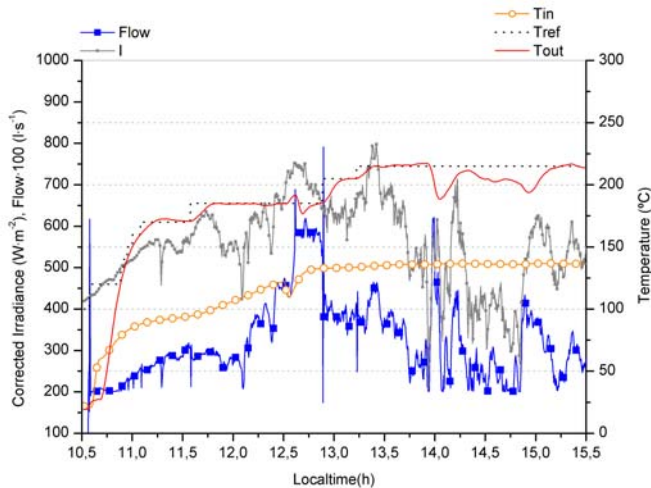


Fig. 10. Test with PID with antireset-windup (07/10/2009)

6. CONCLUSIONS

The design of a robust control scheme has been presented in this paper to control the outlet temperature of a solar collector field despite system uncertainties and disturbances. First, a nonlinear series feedforward was used to compensate for the disturbances effect, and then a set of uncertain linear systems was obtained capturing the system dynamics in the form of an uncertain second-order system plus dead time. Afterwards, the QFT technique was used to design a robust control structure fulfilling different robust time-domain and system stability specifications, and resulting in a robust 2DoF scheme with a reference prefilter and a PID with fixed parameters. A modified antireset-windup scheme plus a reference governor was used to face input saturation problem. The

proposed control structure was tested through several real experiments showing promising results. Future works are focused on studying the robust stability in presence of process saturation, which is a current research field in the QFT framework for systems with dead time.

REFERENCES

- Ajona, J. (1998). *Solar Thermal Electricity Generation (1st chapter)*. CIEMAT, Madrid.
- Álvarez, J., Yebra, L., and Berenguel, M. (2007). Repetitive control of tubular heat exchangers. *Journal of Process Control*, 17, 689–701.
- Álvarez, J., Yebra, L., and Berenguel, M. (2009). Adaptive repetitive control for resonance cancellation of a distributed solar collector field. *International Journal of Adaptive Control Signal Processing*, 23, 331–352.
- Åström, K. and Hägglund, T. (2005). *Advanced PID Control*. ISA - The Instrumentation, Systems, and Automation Society, Research Triangle Park, NC 27709.
- Berenguel, M., Camacho, E., and Rubio, F. (1994). Simulation software package for the acurex field. Technical report, Dep. Ingeniería de Sistemas y Automática, University of Seville (Spain). www.esi2.us.es/~rubio/libro2.html.
- Camacho, E., Berenguel, M., and Rubio, F. (1997). *Advanced Control of Solar Plants (1st edn)*. Springer, London.
- Camacho, E., Rubio, F., Berenguel, M., and Valenzuela, L. (2007a). A survey on control schemes for distributed solar collector fields. part i: modeling and basic control approaches. *Solar Energy*, 81, 1240–1251.
- Camacho, E., Rubio, F., Berenguel, M., and Valenzuela, L. (2007b). A survey on control schemes for distributed solar collector fields. part ii: advances control approaches. *Solar Energy*, 81, 1252–1272.
- Carmona, R. (1985). *Análisis, Modelado y Control de un Campo de Colectores Solares Distribuidos con Sistema de Seguimiento en un Eje*. PhD Thesis, Universidad de Sevilla, Sevilla.
- Cirre, C., Moreno, J., and Berenguel, M. (2003). Robust qft control of a solar collectors field. In D. Martínez (ed.), *IHP Programme, Research results at PSA within the year 2002 access campaign*, 27–33. CIEMAT.
- Cirre, C., Valenzuela, L., Berenguel, M., and Camacho, E. (2004). Control de plantas solares con generación automática de consignas. *RIAI - Revista Iberoamericana de Automática e Informática Industrial*, 1, 50–56.
- de la Parte, M.P., Cirre, C., Camacho, E., and Berenguel, M. (2008). Application of predictive sliding mode controllers to a solar plant. *IEEE Transactions on Control Systems Technology*, 16, 819–825.
- Horowitz, I. (1993). *Quantitative Feedback Design Theory (QFT)*. QFT Publications, Colorado.
- Meaburn, A. and Hugues, F. (1993). Resonance characteristics of distributed solar collector fields. *Solar Energy*, 51, 215–221.
- Meaburn, A. (1995). *Modeling and control of a distributed solar collector field*. Ph.D. thesis, PhD Thesis, The Department of Electrical Engineering and Electronics, UMIST, UK.
- Moreno, J., Berenguel, M., Rodríguez, F., and Banos, A. (2002). Robust control of greenhouse climate exploiting measurable disturbances. *Proceedings of the 15th IFAC World Congress*. Barcelona, Spain.
- Nordgren, R. and Franchek, M. (1994). New formulations for quantitative feedback theory. *International Journal of Robust and Nonlinear Control*, 4, 47–64.
- Ortega, M., Rubio, F., and Berenguel, M. (1997). An h_∞ controller for a solar power plant. *Proceedings of the IASTED International Conference on Control*, 122–125. Cancún, México.
- Roca, L., Berenguel, M., Yebra, L., and Alarcón, D. (2008). Solar field control for desalination plants. *Solar Energy*, 82, 772–786.
- Rubio, F., Gordillo, F., and Berenguel, M. (1996). Lqg/ltr control of the distributed collector field of a solar power plant. *Proceedings of the 13th World Congress of IFAC*, 133–138. San Francisco, USA.